Pseudomorphic GeSn/Ge(001) quantum wells: Examining indirect band gap bowing

Alexander A. Tonkikh, Christian Eisenschmidt, Vadim G. Talalaev, Nikolay D. Zakharov, Joerg Schilling, Georg Schmidt, and Peter Werner

Citation: Appl. Phys. Lett. **103**, 032106 (2013);
View online: https://doi.org/10.1063/1.4813913
View Table of Contents: http://aip.scitation.org/toc/apl/103/3
Published by the American Institute of Physics

Pseudomorphic GeSn/Ge(001) quantum wells: Examining indirect band gap bowing

Alexander A. Tonkikh,[1,2,a)] Christian Eisenschmidt,[3] Vadim G. Talalaev,[1,4] Nikolay D. Zakharov,[1] Joerg Schilling,[4] Georg Schmidt,[3] and Peter Werner[1]
[1]*Max Planck Institute of Microstructure Physics, Weinberg 2 D-06120, Halle (Saale), Germany*
[2]*Institute for Physics of Microstructures RAS, GSP-105, Nizhniy Novgorod, Russia*
[3]*Institute of Physics, Martin Luther University Halle-Wittenberg, Von-Danckelmann-Platz 3 D-01620, Halle (Saale), Germany*
[4]*ZIK SiLi-Nano, Martin Luther University Halle-Wittenberg, Karl-Freiherr-von-Fritsch-Str. 3 D-06120, Halle (Saale), Germany*

(Received 10 May 2013; accepted 29 June 2013; published online 17 July 2013)

A study of the bandgap character of compressively strained $GeSn_{0.060\text{-}0.091}$/Ge(001) quantum wells grown by molecular beam epitaxy is reported. The built-in strain in GeSn wells leads to an increased separation between L and Γ conduction band minima. The prevalent indirect interband transitions in GeSn were probed by photoluminescence spectroscopy. As a result we could simulate the L-valley bowing parameter in GeSn alloys, $b_L = 0.80 \pm 0.06$ eV at 10 K. From this we conclude that even compressively strained GeSn/Ge(001) alloys could become direct band gap semiconductors at the Sn-fraction higher than 17.0 at. %. © *2013 AIP Publishing LLC*.
[http://dx.doi.org/10.1063/1.4813913]

Si optoelectronics and photonics require an efficient light source, which can be integrated with silicon based circuits.[1] One solution to the problem is the integration of III-Vs-based light sources with silicon.[2] Despite a considerable progress in this approach,[3] the search for all-group-IV light emitters remains relevant. A principal material to combine with silicon is therefore germanium. There are three important points in the band structure of Ge which determine its optical character: the valence band maximum at the Γ-point, the conduction band minimum at the L-point (L-valley), and the local conduction band minimum at the Γ-point (Γ-valley). Since the L-valley lies energetically slightly lower than the Γ-valley, Ge is an indirect semiconductor exhibiting low luminescence. One of the recent successful attempts in this direction explores the effect of the tensile strain on the Ge band structure.[4] The tensile strain lowers the Γ-valley minimum faster than the L-valley minimum. Therefore, the tensile-strained Ge can become a direct band gap semiconductor. Another way to obtain a direct band gap in Ge-based materials is to use metastable GeSn alloys.[5] Unstrained $Ge_{1-x}Sn_x$ becomes a direct band gap semiconductor at a Sn-fraction between 6 and 11 at. %.[5–10] Both indirect ($L^+_6 \rightarrow \Gamma^+_8$) and direct ($\Gamma^-_7 \rightarrow \Gamma^+_8$) gaps deviate from Vegard's law[6,7] following a quadratic dependence on the Sn-fraction (x) with a bowing parameter (b_g)[5]

$$E_g(Ge_{1-x}Sn_x) = E_g(Ge)(1-x) + E_g(\alpha Sn)x - b_g x(1-x), \quad (1)$$

where E_g(Ge) and E_g(αSn) are direct or indirect band gaps of Ge and α-Sn, respectively. The direct band gap bowing parameter was found experimentally, $b_\Gamma(300\,K) \sim 2.0$ eV.[8–10] The indirect band gap bowing was simulated by different groups in several publications.[7,11] In particular, in Ref. 7 it was found that $b_{L,theor}$ amounts to 0.89 eV.

For light emitting structures, defect free pseudomorphically grown GeSn/Ge(001) structures are of specific interest. Since the GeSn-crystal structure is tetragonally distorted in these structures, both Sn-content and strain have an impact on the band gap character. Recent reports state that the elastic compressive strain results in the divergence between L and Γ conduction band minima due to a higher value of the Γ-valley deformation potential, making the indirect-direct band gap transition impossible at 300 K.[11]

Here we investigate this claim further. We determine the indirect band gap energies for compressively strained $Ge_{1-x}Sn_x$-layers of different compositions using photoluminescence spectroscopy (PL) at low temperatures. A comparison with experimental values for the direct band gap is then carried out. Finally, we predict that even the compressively strained GeSn layers become direct band gap semiconductors at a certain Sn-fraction.

Four samples of a Ge/GeSn/Ge heterostructure having different Sn-fractions were studied. They were grown by molecular beam epitaxy (MBE) on undoped Ge(001) substrates using a MBE setup SIVA-45 by RIBER. Ge and Sn were evaporated using an electron beam evaporator and an effusion SUMO®-cell, respectively. The deposition rates were 20 pm/s and 2.9 pm/s for Ge and Sn, respectively. The Sn deposition rate was preliminary found using a secondary mass spectroscopy measurement on a δ-Sn layer in Ge. The samples under investigation consist of a 15–18 nm thick GeSn layer sandwiched between a 50 nm thick Ge buffer layer and a 50 nm thick Ge capping layer. The samples were grown using modulations of the growth temperature. The buffer and the capping layers were grown at the temperature of 450 °C, while the GeSn layer was grown at the temperature of 150 °C to reduce the Sn segregation. The accuracy of the growth temperatures was in the range ±10 °C. It was

a)Author to whom correspondence should be addressed. Electronic mail: tonkikh@mpi-halle.de

provided by a preliminary calibration using a thermocouple mounted to the same Ge wafers as used in this study. In order to get sharp heterojunctions, the growth of GeSn layers was performed as described below. First, a monolayer thick Sn layer was deposited onto the buffer layer surface. Then, the deposition of Ge and Sn was performed alternatively. The variation of the Sn-fraction in the as-grown GeSn layer was achieved by changing the ratio of deposited amounts of Sn and Ge. This ratio was increased from 0.06 up to 0.08 for the samples 1-4. The GeSn layers grown in this way are defect-free and uniform in the composition as confirmed by the structural investigations and discussed below.

The structural parameters of all samples were investigated by transmission electron microscopy (TEM) and high resolution X-ray diffractometry (HRXRD). The thickness of the GeSn quantum wells (QW) and the crystal structure were studied using CM20, JEM4010, and TITAN 80/300 electron microscopes in the cross-section geometry. The energy-dispersive X-ray analysis (EDX) was carried out on the GeSn layers by TITAN 80/300 electron microscope equipped with an EDX detector. The XRD-investigation was performed using a Bruker high resolution diffractometer D8 with a mirror and a channel cut monochromator for Cu $K_{\alpha 1}$ radiation and a Vantec detector. Both omega/2theta scans and a reciprocal space mapping (RSM) were performed, respectively, for the Ge 004 and 115+ reflections. The 115+ RSM was used to determine the degree of strain relaxation in the samples. The omega/2theta scans were used to determine the Sn-fraction in the GeSn layers by a fit with the Leptos program (Bruker).

The luminescence properties of GeSn QWs were investigated by using PL spectroscopy in a cryostat cooled down to 10 K. The samples were excited by a 488 nm line of an Ar^+ laser at a power density of 20 W/cm^{-2}. The PL spectra were recorded using a LN2-cooled InGaAs detector having the long-wavelength detection limit of 2400 nm.

An overview of the samples is shown in Table I. As an example of the structural characterization, the cross-section TEM image of the sample 4 is shown in Fig. 1. The dark horizontal bar represents the GeSn layer. The thickness of the GeSn layer deduced from this image amounts to 17.7 ± 0.5 nm. Fig. 1 reveals sharp heterointerfaces of the GeSn layer. The EDX analysis has revealed that our samples contain only Ge and Sn. The GeSn layers were found to be defect-free: no dislocations, stacking faults, or Sn-precipitates were detected by TEM in all four GeSn samples. As an evidence of a cubic crystal structure of GeSn layers, we show a Fourier-transformed image of a high-resolution TEM image taken out of the GeSn layer. This image is inset in Fig. 1 showing only cubic phase reflections.

TABLE I. Experimental parameters of the samples.

Sample	GeSn QW width (TEM) (nm)	GeSn z-direction lattice parameter (XRD) (Å)	Sn-fraction in GeSn QW (at. %)	10 K-luminescence GeSn peak position (PL) (eV)
1	15.1	5.761	6.0	0.654
2	17.5	5.776	6.8	0.624
3	17.3	5.789	7.6	0.615
4	17.7	5.815	9.1	0.584

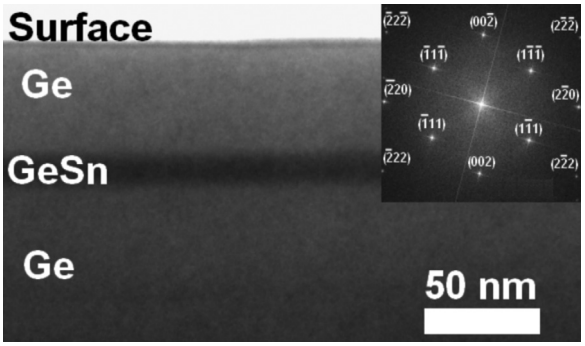

FIG. 1. Cross-section TEM image of the sample 4 taken in the [110] crystallographic direction. The inset shows a picture of the Fourier-transformation of high-resolution TEM image taken out of the GeSn layer and surrounding Ge matrix. The spots correspond to diffraction on a cubic lattice only.

A RSM image of the sample 1 is shown in Fig. 2(a). The reciprocal coordinates correspond to the growth direction [001] (Qz) and to the in-plane direction [110] (Qx). The

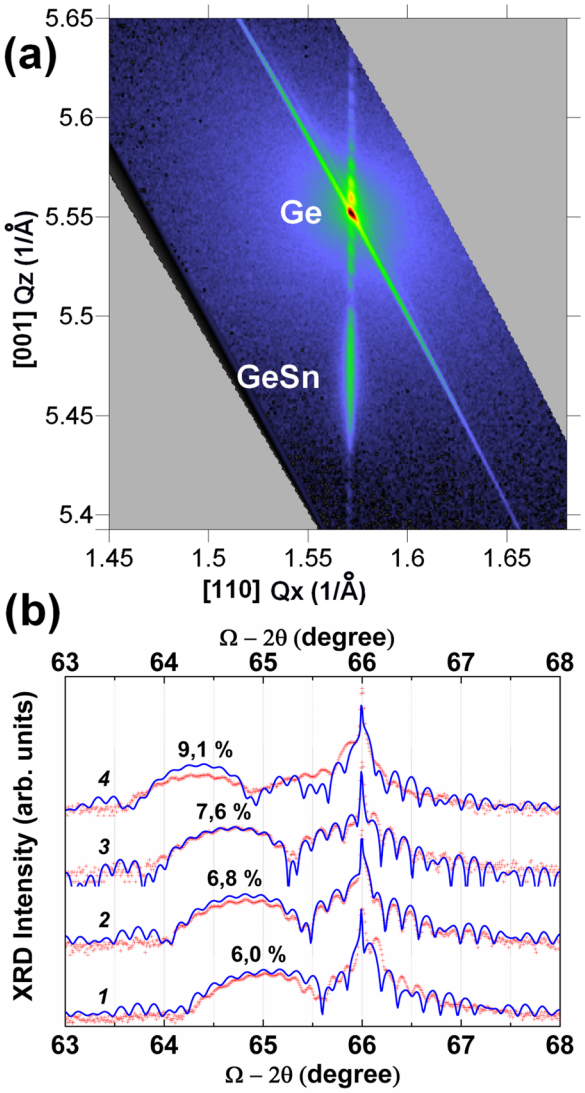

FIG. 2. (a) Reciprocal space map of the sample 1 using the asymmetric 115+ reflection; (b) symmetric 004 omega/2theta scans of the samples 1–4 are given by red symbols. Blue curves are obtained as a result of the simulation within the Leptos program of the experimental XRD-scans. The broad peak of the GeSn layer is modulated by the thickness fringes of the Ge capping layer.

bright spot at the point (1.57; 5.55) is attributed to the substrate. Several additional spots appear as a periodic repetition next to the substrate spot along the Qz direction but at the same Qx-point. We attribute these peaks to thickness fringes of the Ge capping layer due to a reflection from top and bottom of the layer. In addition to these periodic spots, a broad single band is found at lower Qz numbers. We attributed this band to the GeSn layer concluding that the GeSn layer is pseudomorphic, since the substrate peak and GeSn peak are aligned along the Qz-direction. The RSM of the other samples look similar.

To determine the Sn-fractions of the GeSn-layers accurately, the tetragonal elongation of the GeSn unit cell can be exploited. Omega/2theta XRD-scans were used to determine the change in the lattice constant along the z-direction. Fig. 2(b) shows a comparison of the omega/2theta scans with the corresponding Leptos-simulations. Qualitatively, the increase in the Sn-fraction leads to a shift of the GeSn peak away from the substrate peak. The Sn-fraction in the samples 1–4 is increased monotonically up to 9.1 at. %. The error bars are less than 0.1 at. %. The lattice parameter of unstrained GeSn was simulated within the elasticity theory. A bowing of the GeSn lattice parameter from Vegard's law (bowing parameter $b_a = 0.166$ Å) reported in Ref. 12 was taken into account to this simulation.

The PL spectra of the investigated samples and a reference Ge substrate-sample measured at 10 K are presented in Fig. 3. The spectrum of the substrate shows two pronounced features. One peaked at 1744 nm is related to the LA-phonon assisted indirect interband recombination in the Ge bulk.[13]

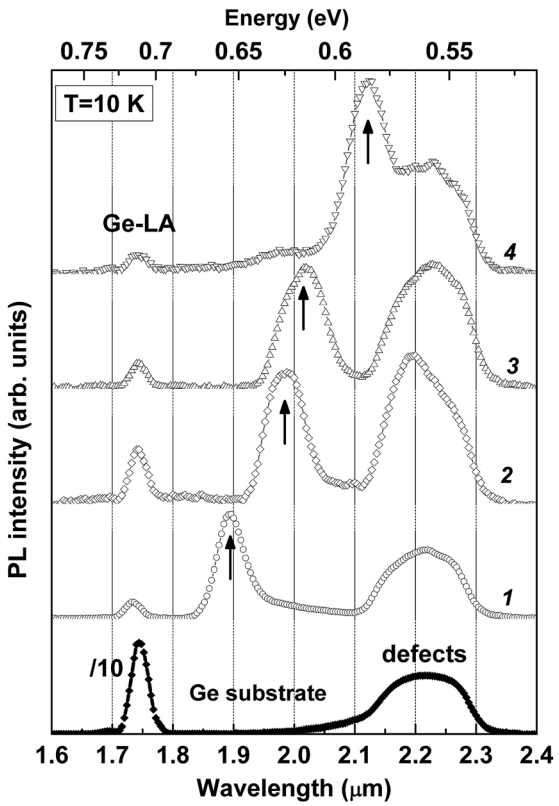

FIG. 3. PL spectra of the samples 1–4 are marked with corresponding numbers; the spectrum of a Ge(001) substrate is the lowest curve. The arrows show positions of GeSn PL peaks. The spectra were taken at 10 K.

The other broad band at longer wavelengths is attributed to a radiative recombination via various defect states in the Ge substrate.[14] Apart from these two features originating from the substrate, the PL-spectra of the GeSn samples contain an additional spectral band. This band with a full width at half maximum below 22 meV is located between the Ge-band gap peak and the peak of defects. The position of this band shifts monotonically to longer wavelengths with increasing Sn-fraction. Therefore, we attribute this peak to the indirect interband radiative transitions between L-valley electron states and heavy hole states within the GeSn QWs. To obtain the indirect band gap energies for compressively strained GeSn from our PL-measurements, one still has to consider two contributions: (a) the confinement energies due to the quantum well character of the GeSn-layers and (b) the phonon energy, in case a phonon is emitted during the indirect emission process.

The confinement energy offsets the quantum well ground states from the band edge energies of the GeSn material and can be well estimated by $E^0_{e(h)} = \hbar^2/(2\,m^*_{e(h)}d^2)$, where $\hbar$ is the reduced Plank constant, $m^*_{e(h)}$ the effective mass of an L-valley electron, or a heavy hole, d the QW thickness. With effective masses taken from Ref. 15 the ground state energy for confined L-electrons calculated for our QWs are 5.0 meV and 3.8 meV in the samples 1 and 2–4, respectively. The values of the ground state energy calculated for heavy holes are 7.5 meV and 5.5 meV for QWs in the samples 1 and 2–4, respectively. As the confinement energies widen the gap between valence and conduction band edges, they have to be subtracted from the PL-energies to obtain the band gap of GeSn. The advantage of using wide QWs is that the error bars in defining these quantum confinement energies due to QW width are less than 1 meV.

The radiation process in GeSn QWs could be accompanied with the emission of a phonon or could occur without any contribution of a phonon.[16] The PL spectra alone do not allow distinguishing between the phonon-assisted and phononless processes. For the beginning we consider a phononless process. This assumption represents a conservative low energy boundary for the indirect band gap of the compressively strained GeSn-layers—a fact we discuss again at end.

So the experimentally determined values for the indirect band gap of $Ge_{1-x}Sn_x$ for the 4 different investigated Sn-fractions are plot as circles in the band gap diagram in Fig. 4.

To be able to extrapolate the Sn-fraction x at which even compressively strained $Ge_{1-x}Sn_x$ alloys become direct band gap semiconductors, we consider the well developed band gap modeling of strained GeSn(Si) alloys[5,9,11] and follow a classical procedure from Ref. 17.

Considering strained GeSn alloys, the direct (E^{ε}_{Γ}) and indirect (E^{ε}_{L}) band gaps were simulated as follows:

$$E^{\varepsilon}_{\Gamma} = E^{R}_{\Gamma} + (a_{\Gamma} - a_V)(\varepsilon_{\perp} + 2\varepsilon_{II}) + b(\varepsilon_{\perp} - \varepsilon_{II}), \quad (2a)$$

$$E^{\varepsilon}_{L} = E^{R}_{L} + (a_{L} - a_V)(\varepsilon_{\perp} + 2\varepsilon_{II}) + b(\varepsilon_{\perp} - \varepsilon_{II}). \quad (2b)$$

Here E^R_Γ and E^R_L are the direct and indirect band gaps of relaxed GeSn given by Eq. (1); a_V, a_Γ, and a_L are deformation potentials of subsequent valleys, and b the shear deformation potential for a strain of tetragonal symmetry. The strain tensor in tetragonally distorted cubic crystals is given

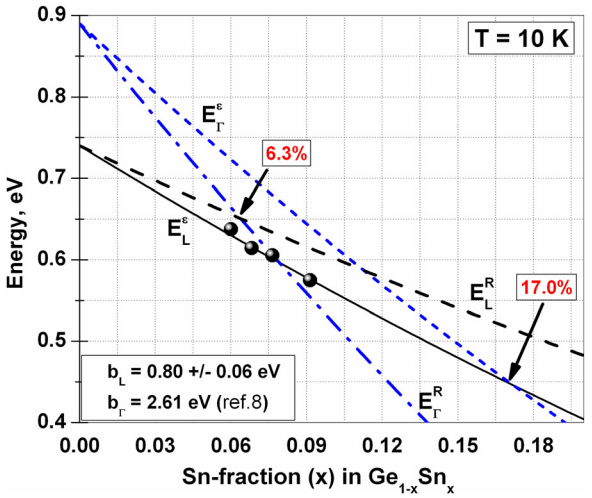

FIG. 4. Energy gaps of pseudomorphic and relaxed GeSn alloys. Circles represent indirect band gap of the samples 1–4; error bars to these data points are several times smaller than the size of circle symbols; solid and dashed lines display the indirect band gaps in pseudomorphic (E_L^ε) and relaxed (E_L^R) GeSn, respectively; short-dashed and dotted-dashed lines display the direct band gaps in pseudomorphic (E_Γ^ε) and relaxed (E_Γ^R) GeSn, respectively.

by the diagonal elements ε_{II} for two in-plane components and $\varepsilon_\perp$ for the normal component to the GeSn QW plane. The latter parameters are functions of elastic constants and the Sn-fraction.

The following material parameters were used in these simulations. The direct and indirect band gaps of Ge are given by $E_g^\Gamma(Ge) = 0.89\,\text{eV}$ and $E_g^L(Ge) = 0.74\,\text{eV}$, respectively. Consequently, $E_g^\Gamma(Sn) = -0.41\,\text{eV}$ (Ref. 18) and $E_g^\Gamma(Sn) = 0.09\,\text{eV}$ (Ref. 19) are the direct and indirect band gaps of α-Sn, respectively. The Γ-valley bowing parameter $b_\Gamma(10\,\text{K}) = 2.61\,\text{eV}$ (Ref. 8). Furthermore, a set of structural parameters of Ge and α-Sn (lattice parameters, elastic constants) was taken from the handbook.[15] A set of deformation potentials was chosen in the same way as described by Chang *et al.*[20] Besides discussed above physical values, all other parameters for GeSn alloys were interpolated according to Vegard's law. This leaves the L-valley bowing parameter (b_L) as the single remaining fitting parameter in this simulation. The best fit for the L-valley bowing parameter is achieved with $b_L = 0.80 \pm 0.06\,\text{eV}$. The correct determination of the bowing parameter b_L is not only important for the strained GeSn-layers. The same bowing parameter appears also in the unstrained (relaxed) version of the band gap calculation (Eq. (1)). The resulting plots of the energy gaps for compressively strained as well as for relaxed GeSn alloys including our experimentally determined value are summarized in Fig. 4.

Taking into account our newly determined L-valley bowing parameter and the reported Γ-valley bowing ($b_\Gamma = 2.61\,\text{eV}$) it follows, the pseudomorphic GeSn/Ge(001) alloys may have a direct band gap at Sn-fractions higher than 17.0 at. % for temperatures around 10 K. Regarding the unstrained alloys, the indirect-to-direct crossover may occur at a Sn-fraction of 6.3 at. % at 10 K. The latter value is consistent with the experimental crossover found at about 7 at. % in Ref. 21.

Up to here we did not consider a phonon contribution to the radiative transitions within the GeSn QWs. If we assume that our PL-spectra measured the phonon assisted optical transitions in the GeSn QWs so that a phonon is emitted together with every photon, then the real indirect band gap energies are even higher than the ones considered up to now. This will lead to a decrease in the fitted L-valley bowing parameter. For instance, the assumption of the emission of the Ge-LA phonon having the energy of 28 meV leads to a value of $b_L^* = 0.17 \pm 0.06\,\text{eV}$. Subsequently, the indirect-direct band gap transition would occur at 9.4 at. % and 4.8 at. % for the pseudomorphic and relaxed GeSn alloys, respectively. The latter more "optimistic" value of the indirect-direct band gap transition deviates much from that generally assumed for GeSn alloys. Thereby, an additional evidence of the indirect-direct band gap transition for pseudomorphic GeSn/Ge(001) would be of fundamental and practical importance.

Possible further adjustments of the experimentally determined band gap energies, e.g., by a contribution of the exciton binding energy (4.6 meV (Ref. 8)) or by a lower value of the GeSn lattice bowing parameter reported in Ref. 22 are already within the error bars of our considered values.

In conclusion our investigation predicts a direct band gap for pseudomorphic GeSn/Ge(001) semiconductor structures at a Sn-fraction higher than 17 at. %. The latter composition is accessible by means of epitaxial growth techniques. These pseudomorphic layers could serve as active regions in light emitting devices in Ge-photonic circuits based on germanium-on-insulator substrates.

A.A.T. gratefully acknowledges the financial support of the Federal Ministry for Education and Research (BMBF) within the WING-project. V.G.T. and J.S. would like to thank the BMBF for financial support within the Centre for Innovation Competence SiLi-nano (Project No. 03Z2HN12). Authors acknowledge the technical support of A. Frommfeld, S. Hopfe, and C. Münx.

[1]R. Soref, Nat. Photonics **4**, 495 (2010).
[2]H. Park, A. W. Fang, S. Kodama, and J. E. Bowers, Opt. Express **13**, 9460 (2005).
[3]R. W. Kelsall, Nat. Photonics **6**, 577 (2012).
[4]J. Liu, L. C. Kimerling, and J. Michel, Semicond. Sci. Technol. **27**, 094006 (2012).
[5]J. Kouvetakis, J. Menendez, and A. V. G. Chizmeshya, Annu. Rev. Mater. Res. **36**, 497 (2006).
[6]G. He and H. A. Atwater, Phys. Rev. Lett. **79**, 1937 (1997).
[7]W.-J. Yin, X.-G. Gong, and S.-H. Wei, Phys. Rev. B **78**, 161203(R) (2008).
[8]V. R. D'Costa, C. S. Cook, A. G. Birdwell, C. L. Littler, M. Canonico, S. Zollner, J. Kouvetakis, and J. Menéndez, Phys. Rev. B **73**, 125207 (2006).
[9]H. Lin, R. Chen, W. Lu, Y. Huo, T. I. Kamins, and J. S. Harris, Appl. Phys. Lett. **100**, 102109 (2012).
[10]J. Mathews, R. T. Beeler, J. Tolle, C. Xu, R. Roucka, J. Kouvetakis, and J. Menéndez, Appl. Phys. Lett. **97**, 221912 (2010).
[11]S. Gupta, B. Magyari-Köpe, Y. Nishi, and K. C. Saraswat, J. Appl. Phys. **113**, 073707 (2013).
[12]P. Aella, C. Cook, J. Tolle, S. Zollner, A. V. G. Chizmeshya, and J. Kouvetakis, Appl. Phys. Lett. **84**, 888 (2004).
[13]R. R. Lieten, K. Bustillo, T. Smets, E. Simoen, J. W. Ager III, E. E. Haller, and J.-P. Locquet, Phys. Rev. B **86**, 035204 (2012).
[14]S. Shevchenko and A. Tereshchenko, Phys. Status Solidi C **4**, 2898 (2007).
[15]O. Madelung, M. Schultz, and H. Weiss, *Physics of Group IV Elements and III-V Compounds*, 1st ed. (Springer-Verlag, New York, 1982), Vol. 17a.

[16]D. Dutartre, G. Bremond, A. Souifi, and T. Benyattou, Phys. Rev. B **44**, 11525 (1991).
[17]C. G. Van de Walle, Phys. Rev. B **39**, 1871 (1989).
[18]P. Lawaetz, Phys. Rev. B **4**, 3460 (1971).
[19]C. F. Lavine and A. W. Ewald, J. Phys. Chem. Solids **32**, 1121 (1971).
[20]G.-E. Chang, S.-W. Chang, and S. L. Chuang, IEEE J. Quantum Electron. **46**, 1813 (2010).
[21]R. Chen, H. Lin, Y. Huo, C. Hitzman, T. I. Kamins, and J. S. Harris, Appl. Phys. Lett. **99**, 181125 (2011).
[22]R. Beeler, R. Roucka, A. V. G. Chizmeshya, J. Kouvetakis, and J. Menendez, Phys. Rev. B **84**, 035204 (2011).